Int J Clin Exp Med 2014;7(4):1014-1021
www.ijcem.com /ISSN:1940-5901/IJCEM0000087

Original Article

Quantitative analysis of real-time tissue elastography for evaluation of liver fibrosis

Ying Shi[1], Xing-Hua Wang[1], Huan-Hu Zhang[2], Hai-Qing Zhang[1], Ji-Zheng Tu[1], Kun Wei[1], Juan Li[1], Xiao-Li Liu[3]

[1]Department of Ultrasound, Second Hospital of Shanxi Medical University, Taiyuan 030001, China; [2]Department of Liver Diseases, Second Hospital of Shanxi Medical University, Taiyuan 030001, China; [3]Department of Pathology, Second Hospital of Shanxi Medical University, Taiyuan 030001, China

Received February 25, 2014; Accepted March 22, 2014; Epub April 15, 2014; Published April 30, 2014

Abstract: The present study aimed to investigate the feasibility of quantitative analysis of liver fibrosis using real-time tissue elastography (RTE) and its pathological and molecule biological basis. Methods: Fifty-four New Zealand rabbits were subcutaneously injected with thioacetamide (TAA) to induce liver fibrosis as the model group, and another eight New Zealand rabbits served as the normal control group. Four rabbits were randomly taken every two weeks for real-time tissue elastography (RTE) and quantitative analysis of tissue diffusion. The obtained twelve characteristic quantities included relative mean value (MEAN), standard deviation (SD), blue area % (% AREA), complexity (COMP), kurtosis (KURT), skewness (SKEW), contrast (CONT), entropy (ENT), inverse different moment (IDM), angular secon moment (ASM), correlation (CORR) and liver fibrosis index (LF Index). Rabbits were executed and liver tissues were taken for pathological staging of liver fibrosis (grouped by pathological stage into S0 group, S1 group, S2 group, S3 group and S4 group). In addition, the collagen I (Col I) and collagen III (Col III) expression levels in liver tissue were detected by Western blot. Results: Except for KURT, there were significant differences among the other eleven characteristic quantities ($P < 0.05$). LF Index, Col I and Col III expression levels showed a rising trend with increased pathological staging of liver fibrosis, presenting a positive correlation with the pathological staging of liver fibrosis ($r = 0.718$, $r = 0.693$, $r = 0.611$, $P < 0.05$). Conclusion: RTE quantitative analysis is expected for noninvasive evaluation of the pathological staging of liver fibrosis.

Keywords: Ultrasound, elastography, liver fibrosis, non-invasive diagnosis

Introduction

Liver fibrosis is not only the common pathological outcome of various chronic liver injuries, but also an early reversible link in the progressive development of chronic liver diseases. It is mainly characterized by abnormal excessive deposition of extracellular matrix (ECM), which could be further developed into liver cirrhosis [1, 2]. Early diagnosis and timely treatment of liver fibrosis can significantly improve the prognosis of chronic liver diseases. Due to the current lack of non-invasive method of early diagnosis with strong sensitivity and high specificity, it has become one of the hotspots to explore non-invasive examination that can dynamically monitor liver fibrosis.

Diagnosis of liver fibrosis mainly relies on three means: histopathology, Serological test and imaging technique [3]. Liver histopathological biopsy is the gold standard for the diagnosis of liver fibrosis, but it is an invasive inspection, with poor reproducibility. The specificity, sensitivity and accuracy of serological liver fibrosis indexes for the diagnosis of liver fibrosis can not reflect the actual situation of liver fibrosis yet. As an important imaging diagnostic mean, ultrasound has become an important method of imaging diagnosis for liver fibrosis due to its simple and economical detection method and dynamic observation. In recent years, the ultrasound elastography technique marked by ultrasound biomechanics has been rapidly developed [4], demonstrating good clinical application prospect in quantifying the degree of liver fibrosis and evaluating the pathological staging, so that it is considered as a non-invasive, rapid, repeated method for quantitative detection of liver fibrosis. In this study, real-time tissue elas-

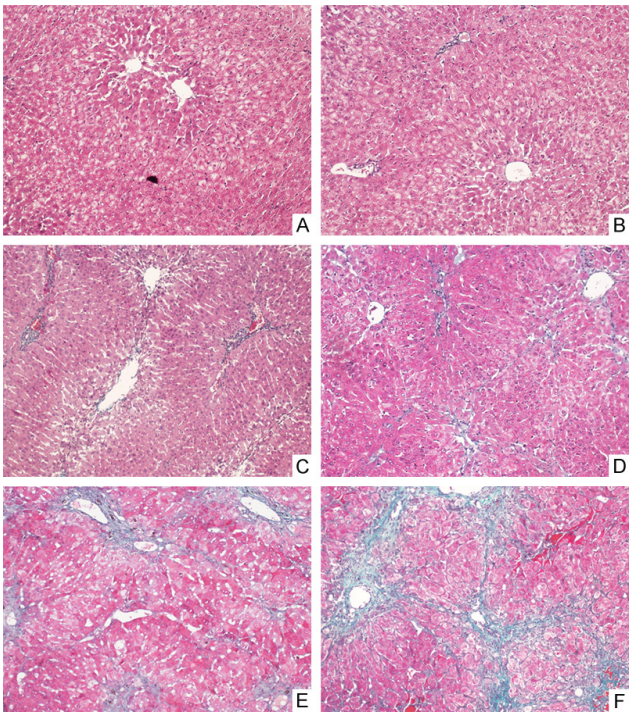

Figure 1. Masson staining pathology images of rabbit liver tissues (× 100): A: normal control group, with normal liver tissue. B: S0 group: within S0 stage, without fibrosis. C: S1 group: within S1 stage, with periportal fibrosis enlargement limited sinus and lobular fibrosis. D: S2 group: within S2 stage, with periportal fibrosis, formation of fibrous septum and reservation of lobular structure. E: S3 group: within S3 stage, with fibrous septum and lobular structural disorder, without liver cirrhosis. F: S4 group: within S4 stage, with early cirrhosis and formation of pseudolobule.

tography (RTE) technique was used to detect the pathological staging of rabbit liver fibrosis, so as to explore the molecule biological basis.

Materials and methods

Reagents

Thioacetamide (TAA, Sigma Alorich), Collagen I mouse monoclonal antibody (ab90395), and Collagen III mouse monoclonal antibody (MAB6614); Protein Extraction Kit and Protein Quantification Kit (Beijing Puli Lai Gene Technology Co., Ltd.), ECL chemiluminescence kit (Thermo Scientific), and β-actin mouse monoclonal antibody (sc-47778).

Animals and modeling

There were a total of sixty-two New Zealand rabbits, including half male and half female, weighed 2~3 kg. They were randomly divided into two groups, including the normal control group (8) and the model group (54). The model group was given subcutaneous injection of 4% TAA (dose of 1.0 ml/kg), two times/week for 20 weeks.

Instrument

Hitachi's HI Vision Preirus ultrasound diagnostic unit with L52 linear array probe with a frequency of 7.5 MHz was selected, equipped with RTE technology and software for quantitative analysis of tissue diffusion.

Protocols

Four rabbits were taken for ultrasound elastography examination every two weeks. The rabbits were then executed, and the 1 × 1 × 1 cm^3 rabbit liver tissues were taken, which were fixed with 10% formalin solution for histopathological examination. In addition, other liver tissues were frozen in liquid nitrogen at -80°C for detection of Col I and Col III contents by Western blot. The study was approved by the Animal Care and Use Committee at the Shanxi Medical University.

Ultrasound elastography

After anesthesia, rabbit hairs in the liver region were removed. The rabbits were set orthostaticly to significantly reduce the impact of breathing on elastography. The left lobe of liver below the xiphoid was selected in order to avoid the intrahepatic large vessels, 0.5~1.0 cm away from the liver capsule, with a depth of 4 cm. The region of interest (ROI) was with the perimeter of 46.1 mm and the area of 1.3 cm^2. A good two-dimensional slice was taken, and the elastography was converted. The cardiac impulse was used as the external force. The intensity could be displayed through the waveform curves. There were five continuous and stable troughs, one of which was selected for observation of the elastogram (**Figures 1**, **2**). ROI was analyzed using software. The obtained twelve characteristic quantities included relative mean value (MEAN), standard deviation (SD), blue area % (% AREA), complexity (COMP), kurtosis (KURT), skewness (SKEW), contrast (CONT), entropy (ENT), inverse different moment (IDM), angular secon moment (ASM), corre-

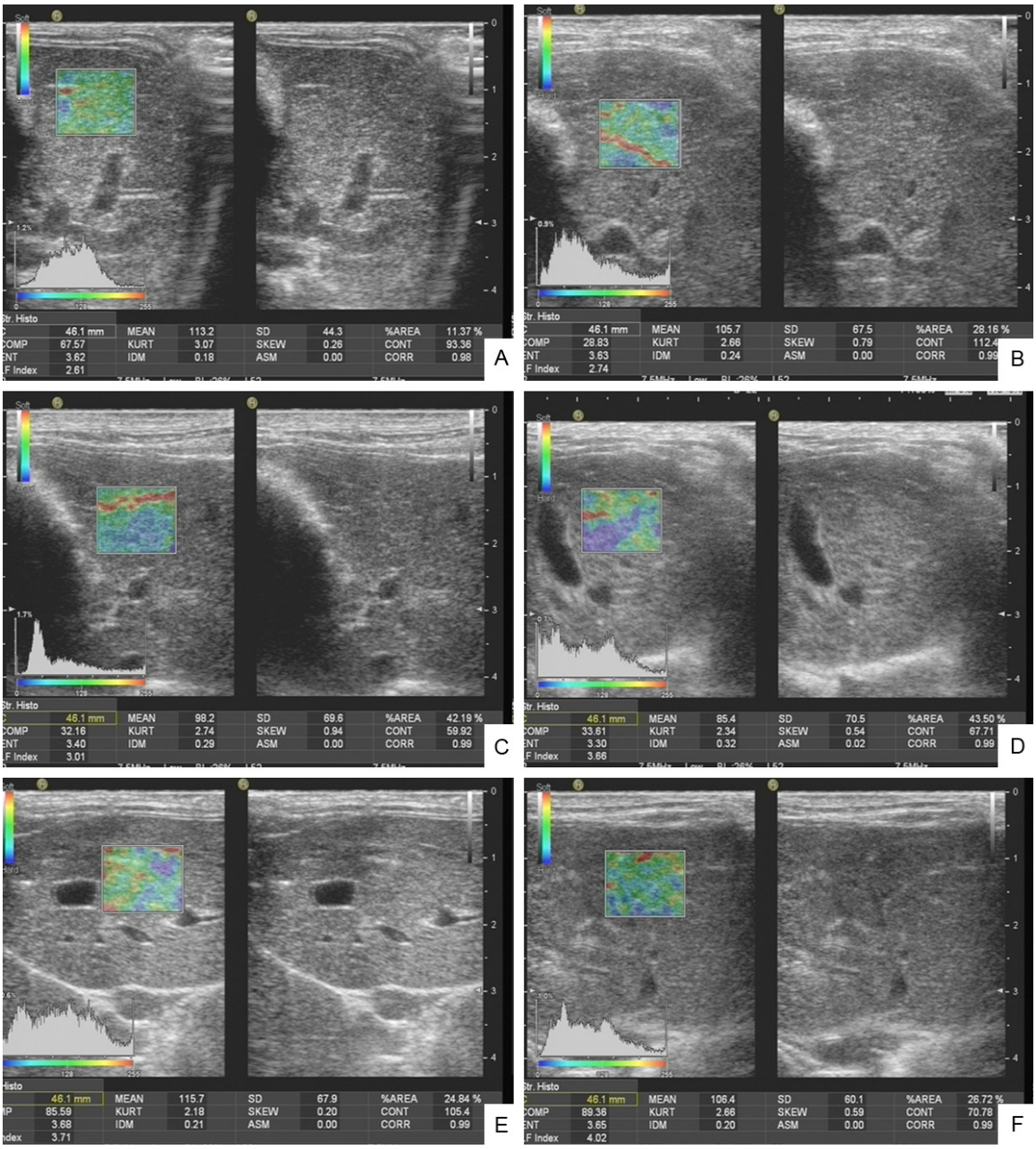

Figure 2. Rabbit elastography images: A: Normal control group. B: S0 group. C: S1 group. D: S2 group. E: S3 group. F: S4 group.

lation (CORR) and liver fibrosis index (LF Index). Each patient was measured for three times and the mean was calculated.

Pathological staging

1 × 1 × 1 cm^3 rabbit liver tissues were taken and fixed with 10% formalin solution, routinely embedded with paraffin serially sectioned, stained with hematoxylin-eosin (HE), reticular fiber and Masson, followed by pathological observation. According to the viral hepatitis prevention and treatment standards jointly revised by the Infectious and Parasitic Diseases Branch, and Hepatology Branch of Chinese Medical Association in 2000 [5], the degrees of liver fibrosis were staged into S0: no fibrosis; S1: periportal fibrosis enlargement, limited sinus and lobular fibrosis; S2: periportal fibrosis, formation of fibrous septum and retainment of lobular structure; S3: fibrous septum

Table 1. ANOVA results of twelve characteristic quantities of New Zealand rabbits

Characteristic Quantities	F Value	*P* Value
MEAN	8.029	0.000
SD	15.632	0.000
% AREA	15.544	0.000
COMP	4.721	0.001
KURT	1.330	0.255
SKEW	5.328	0.000
CONT	3.332	0.007
ENT	3.622	0.004
IDM	7.580	0.000
ASM	2.292	0.049
CORR	2.358	0.044
LF	Index	19.199

Note: MEAN: relative mean value; SD: standard deviation; % AREA: blue area %; COMP: complexity; KURT: kurtosis; SKEW: skewness; CONT: contrast; ENT: entropy; IDM: inverse different moment; ASM: angular secon moment; CORR: correlation; LF Index: liver fibrosis index.

with lobular structural disorder, without liver cirrhosis; S4: early liver cirrhosis.

Western blot detection

50 mg of frozen liver tissues were cut into pieces, added with tissue lysates and ground. The total protein was extracted, added with sample buffer and separated by electrophoresis, followed by transmembrane, blocking, incubation with Col I antibody (1:1000), Col III antibody (1:500) and β-actin antibody (1:1000) overnight at 4°C, incubation with secondary antibody, ECL substrate chemiluminescence, developing, fixing, and scanning. Quantity one image analysis system was used for analysis of the average gray value (*A* value) of each band. The *A* value of target band was divided by the *A* value of internal reference in order to correct the error. The results expressed the relative expression levels of Col I and Col III.

Statistical analysis

SPSS 17.0 statistical software was used. All measurement data were expressed as $\bar{x} \pm s$. One-way analysis of variance (One-Way ANOVA) was used for comparison among groups. Spearman rank correlation analysis was used for correlation analysis. The receiver operating curve (ROC) was constructed. $P < 0.05$ was considered as statistically significant.

Table 2. Correlation between twelve characteristic quantities of New Zealand rabbits and the pathological staging

Characteristic Quantities	r Value	*P* Value
MEAN	-0.462	0.000
SD	0.514	0.000
% AREA	0.546	0.000
COMP	0.317	0.001
KURT	-0.058	0.494
SKEW	0.367	0.000
CONT	0.024	0.773
ENT	-0.317	0.000
IDM	0.470	0.000
ASM	0.247	0.003
CORR	0.237	0.005
LF Index	0.718	0.014

Note: MEAN: relative mean value; SD: standard deviation; % AREA: blue area %; COMP: complexity; KURT: kurtosis; SKEW: skewness; CONT: contrast; ENT: entropy; IDM: inverse different moment; ASM: angular secon moment; CORR: correlation; LF Index: liver fibrosis index.

Results

Pathological staging of rabbit liver fibrosis

There were eight rabbits in the normal control group, and thirty-two rabbits were successfully modeled in the liver fibrosis model group (S1~S4 periods), with the successful modeling rate of 59.3%. Pathological staging: seven in S0 stage, fourteen in S1 stage, six in S2 stage, seven in S3 stage, and five in S4 stage. According to the pathological staging, they were grouped into S0 group, S1 group, S2 group, S3 group and S4 group (**Figure 1**).

Correlation between quantitative parameters of elastography and pathological staging of liver fibrosis

In addition to the KURT ($P > 0.05$), there were statistically significant differences among the other eleven characteristic quantities ($P < 0.05$) (**Table 1**). The correlation between eleven characteristic quantities with statistically significant differences and pathological staging was further analyzed, and the results showed that LF Index, SD and % AREA were with larger positive correlation coefficients (**Table 2**), wherein, LF Index was with the largest correlation ($r = 0.718$, $P < 0.05$) (**Figure 2**).

Table 3. LF Index, % AREA and SD in evaluating the area under the curve (AUC) and cut-off value during different pathological stages

Characteristic Quantities	S ≥ S1		S ≥ S2		S ≥ S3		S = S4	
	AUC	Cut-off Value	AUC	Cut-off Value	AUC	Cut-off Value	AUC	Cut-off Value
LF Index	0.754	2.525	0.945	2.699	0.983	3.107	0.924	3.333
% AREA	0.735	24.905	0.770	25.525	0.794	26.215	0.755	32.170
SD	0.719	60.750	0.718	61.700	0.738	65.050	0.689	65.150

Table 4. LF Index, Col I and Col III expression levels of New Zealand rabbits ($\bar{x} \pm s$)

Group	LF Index	Col I	Col III
Control group	2.33 ± 0.25	0.88 ± 0.68	0.90 ± 0.03
S0	2.50 ± 0.42	0.93 ± 0.61	0.91 ± 0.01
S1	2.42 ± 0.22	1.01 ± 0.10	0.98 ± 0.01
S2	2.77 ± 0.25$^{*,\&}$	1.07 ± 0.03$^{*,\#}$	1.01 ± 0.05$^{*,\#}$
S3	3.45 ± 0.41$^{*,\#,\&,\$}$	1.04 ± 0.06*	1.00 ± 0.08*
S4	3.53 ± 0.28$^{*,\#,\&,\$}$	1.01 ± 0.08$^{*,\#}$	1.00 ± 0.06*
F value	19.199	3.545	2.758
P value	0.000	0.034	0.029

Note: *Compared with the control group, P < 0.05; $^{\#}$compared with S0 group, P < 0.05; $^{\&}$compared with S1 group, P < 0.05; $^{\$}$compared with S2 group, P < 0.05.

Intergroup pairwise comparison of LF Index, % AREA and SD

The correlation coefficient between LF Index, % AREA or SD and pathological stage was relatively larger. The differences of pairwise comparison during different pathological stages were further analyzed, and the results showed that there was statistically significant differences in LF Index between the control group and S2 group, S3 group or S4 group ($P < 0.05$), between S0 group and S3 group or S4 group ($P < 0.05$), between S1 group and S2 group, S3 group or S4 group ($P < 0.05$), between S2 group and S3 group or S4 group ($P < 0.05$). The other groups showed no significant difference between any two groups ($P > 0.05$). There was statistically significant difference in % AREA between the control group and the S1 group, S2 group, S3 group or S4 group ($P < 0.05$), between the S1 group and S3 group or S4 group ($P < 0.05$), between S2 group and S4 group ($P < 0.05$). The other groups showed no significant difference between any two groups ($P > 0.05$). There was statistically significant difference in SD between the control group and S1 group, S2 group, S3 group or S4 group ($P < 0.05$). The other groups showed no significant difference between any two groups ($P > 0.05$).

ROC curve analysis

ROC curve was used to determine LF Index, % AREA and SD for evaluation of the area under the curve (AUC) and cut-off value during different pathological stages (**Table 3**). Among three parameters, LF Index had the best effect in evaluating the pathological staging of liver fibrosis, followed by % AREA.

Western blot assay of the expression level of ECM

With the aggravation of the pathological staging of liver fibrosis, the expression levels of Col I, Col III in liver tissues showed a rising trend overall. The Col I and Col III expression levels in liver tissue were positively correlated to the pathological staging of liver fibrosis ($r = 0.693$, $P < 0.05$; $r = 0.611$, $P < 0.05$). The Col I expression levels in S2 group, S3 group and S4 group were significantly higher than the normal control group, with statistically significant differences ($P < 0.05$); the Col I expression levels in S2 group and S4 group were significantly higher than S0 group, with statistically significant differences ($P < 0.05$). The Col III expression levels in S2 group, S3 group and S4 group were significantly higher than the control group, with statistically significant differences ($P < 0.05$); the Col III expression level in S2 group was significantly higher than S0 group, with statistically significant difference ($P < 0.05$) (**Table 4**).

Discussion

The activation of hepatic stellate cells (HSC) is the central link of liver fibrosis [6]. While liver damage, HSC in a stationary state located in the perisinusoidal Disse cavity is transformed into myofibroblast-like cell (MFBC) with activities of proliferation, contraction and migration, promoting inflammation and fibrogenesis phenotype, followed by synthesis of a large number

of ECM, which are deposited in the liver and caused liver fibrosis, leading to changes in liver stiffness and liver elastic parameters. Therefore, liver elasticity (stiffness) measurement has become a non-invasive method for the diagnosis of liver fibrosis received attention in recent years. The researches showed that the hardness of the liver tissue was related to the degree of liver fibrosis [7-15]. The basic principle of ultrasound elastography was that an internal (including itself) or external dynamic or static (quasi-static) excitement was applied to the tissue, in addition with the use of the probe or probe squeeze plate device, the tissue was longitudinally compressed along the probe. Under the role of elasticity, biomechanics and other physical factors, the tissue would produce a response, such as displacement and strain. The elasticity distribution within tissues could be evaluated by using ultrasonic imaging method and combining with digital signal processing or digital image processing techniques, which could directly or indirectly reflect the differences of the modulus of elasticity and other mechanical properties within the tissue. Transient elastography technique (Fibroscan, FS) is a method widely used currently. A number of studies have been conducted in patients with liver fibrosis, such as chronic hepatitis C [8, 9, 12] and liver fibrosis caused by other etiologies. The diagnostic value has been validated to a certain extent. But for patients with obvious obesity, fatty liver, massive ascites, intercostal space stenosis, acute hepatitis and extra liver biliary obstruction, FS was difficult to succeed and could not directly display the liver image. Compared with FS, RTE technique used in this study [16] was more simple, which could carry out elastography based on two-dimensional ultrasound, visualize the liver ultrasound images, and perform the elasticity detection of the target liver tissue under direct vision in order to obtain quantitative parameters.

Real-time tissue elastography (RTE) is a kind of oppressive elastography technique [16]. Its principle is based on different elastic coefficients of different tissues. Coupled with different strains after force or alternating vibration, different fragment signals were collected during a certain period of time. The combined autocorrelation method (CAM) was used for analysis of the echo signals reflected before and after the oppression. The displacements at different positions within the tissue were estimated to calculate the degree of deformation, and then imaging in grayscale or color encoding. At present, many studies have shown that RTE had achieved a high degree of accuracy in the differential diagnosis of benign and malignant tumors in breast, thyroid and other superficial organs [17, 18]. The new generation of RTE technology was equipped with quantitative analysis of tissue diffusion. Based on the principle of RTE, the imaging solely relied on the tissue compression formed by patient's own cardiovascular pulsatile capability reduced the impact of manual pressure, free from the limitations of intercostal space stenosis, restrictions ascites, fatty degeneration and other factors. The method was performed by using analytical software for analysis of ROI in order to obtained eleven characteristic quantities, including [19] relative mean value (MEAN): the mean value of the relative deformation data within ROI; standard deviation (SD): the standard deviation value of the relative deformation within ROI; blue area % (% AREA): the ratio of pixels of relative deformation below the threshold within ROI; complexity (COMP): the relative deformation within ROI was squared and calculated by the perimeter and area of the blue area; kurtosis (KURT): the asymmetry of deformation data distribution, presenting the characteristic number of peak height in the probability density distribution curve at the mean value; skewness (SKEW): the deviation of deformation data distribution and the mean value, presenting the characteristic number of the degree of asymmetry relative to the mean value in the probability density distribution curve; contrast (CONT): the distribution of deformation data relative to the principal diagonal, that was, the greater the resolution was, the greater the contrast would be; entropy (ENT): the equal degree of deformation data distribution, that was the average amount of information; inverse different moment (IDM): the inorganic deformation of distribution data and the complexity of characteristic quantities' own properties; angular secon moment (ASM): the specific number of pixels set and correlation of the whole data, consistency of the characteristic quantities' textures, and entropy within ROI; correlation (CORR): the directivity of characteristic quantities' textures, reflecting the degree of similarity of characteristic quantities' elements in the row and column directions. These eleven char-

acteristic quantities were calculated by a multiple regression equation, ultimately, the liver fibrosis (LF Index) was obtained for comprehensive reflection of the elastic characteristics of the tissue.

Studies have confirmed that RTE could be used for non-invasive evaluation of liver fibrosis [20-22]. This real-time tissue elastography technique had more obvious advantages than conventional two-dimensional ultrasound and color Doppler ultrasound in evaluating liver fibrosis. This study showed that among twelve characteristic quantities, the correlation between LF Index, SD or % AREA and the pathological staging of liver fibrosis was relatively larger, wherein, LF Index was the maximum ($r = 0.718$, $P < 0.05$). ROC curve analysis also showed that LF Index had the best effect in assess evaluating the pathological staging of liver fibrosis, indicating that as a comprehensive parameter to reflect the elastic characteristics of liver tissue, LF Index could better evaluate the pathological staging of liver fibrosis. The differences of pairwise comparisons of LF Index, SD and % AREA were further analyzed during the pathological stages, and the results showed that LF Index, SD and % AREA were different in distinguishing the differences of different pathological stages, wherein, LF Index, SD and % AREA were all significantly different between the control group and S2 group, between S2 group, S3 group and S4 group, indicating that the elastic parameters could not distinguish the subtle lesions in liver tissue during the S2 stage. If S2 period was considered as the boundary of mild and severe liver fibrosis, the results would show that there was a statistically significant difference in LF Index between S1 group and S2 group, S3 group or S4 group ($P < 0.05$), between S2 group and S3 group or S4 group; there was a statistically significant difference in % AREA between S1 group and S3 group or S4 group ($P < 0.05$), between S2 group and S4 group ($P < 0.05$), indicating that LF Index and % AREA might have potential abilities in distinguishing mild and severe liver fibrosis.

The synthesis and degradation of ECM was in dynamic equilibrium in normal liver tissues. While liver fibrosis, the amount of ECM generation was increased and the amount in degradation was reduced, which caused a large number of ECM deposition in liver tissues, leading to increased liver stiffness and changes in liver elastography parameters. The molecular biology technique could detect the expression level of ECM. The main component of ECM was Collagen I (Col I) and Collagen III (Col III). In this study, Col I and Col III expression levels were detected by Western blot. It was found that Col I and Col III showed a rising trend with the aggravation of liver fibrosis staging, confirming the molecule biological basis of increased LF Index with the aggravation of liver fibrosis staging.

There are also limitations of this study. Rabbit spontaneous breathing had certain impact on the collection of elastic data. In this study, the modeling method of TAA-induced liver fibrosis could cause more obvious liver inflammation and necrosis, which might affect the analysis of the quantitative elastic parameters.

Since animal experiments were carried out in this study, the results were to be clinically proven. It was believed that with extensive researches and clinical practices, RTE quantitative analysis of tissue diffusion was expected for noninvasive evaluation of the degree of liver fibrosis.

Acknowledgements

This study is supported by the Scientific Foundation for Postdoctorates of China (Grant No. 2012M520602), Returned Overseas Students Merit-based Funding for Science and Technology Activities of Shanxi Province (Jin MOHRSS Letter [2013] No. 68), Higher School Science & Technology Development Project of Shanxi Province (Jin UNESCO [2012] No. 15).

Disclosure of conflict of interest

None.

Address correspondence to: Dr. Xing-Hua Wang, Department of Ultrasound, Second Hospital of Shanxi Medical University, 382 Wuyi Road, Taiyuan 030001, China. E-mail: wangxinghuadoc@163.com

References

[1] Fallowfield J and Hayes P. Pathogenesis and treatment of hepatic fibrosis: is cirrhosis reversible? Clin Med 2011; 11: 179-183.

[2] Udell JA, Wang CS, Tinmouth J, FitzGerald JM, Ayas NT, Simel DL, Schulzer M, Mak E and Yoshida EM. Does this patient with liver disease have cirrhosis? JAMA 2012; 307: 832-842.

[3] Pinzani M. Noninvasive methods for the assessment of liver fibrosis: a window open on the future? Hepatology 2011; 54: 1476-1477.
[4] Yu H and Wilson SR. New noninvasive ultrasound techniques: can they predict liver cirrhosis? Ultrasound Q 2012; 28: 5-11.
[5] Epidemiology PaHboCMA. Plan for prevention and treatment of viral hepatitis. Chin J Hepatol 2000; 8: 324-329.
[6] Lee UE and Friedman SL. Mechanisms of hepatic fibrogenesis. Best Pract Res Clin Gastroenterol 2011; 25: 195-206.
[7] Alisi A, Pinzani M and Nobili V. Diagnostic power of fibroscan in predicting liver fibrosis in nonalcoholic fatty liver disease. Hepatology 2009; 50: 2048-2049; author reply 2049-2050.
[8] Castera L, Vergniol J, Foucher J, Le Bail B, Chanteloup E, Haaser M, Darriet M, Couzigou P and De Ledinghen V. Prospective comparison of transient elastography, Fibrotest, APRI, and liver biopsy for the assessment of fibrosis in chronic hepatitis C. Gastroenterology 2005; 128: 343-350.
[9] Colletta C, Smirne C, Fabris C, Toniutto P, Rapetti R, Minisini R and Pirisi M. Value of two noninvasive methods to detect progression of fibrosis among HCV carriers with normal aminotransferases. Hepatology 2005; 42: 838-845.
[10] Corpechot C, El Naggar A, Poujol-Robert A, Ziol M, Wendum D, Chazouilleres O, de Ledinghen V, Dhumeaux D, Marcellin P, Beaugrand M and Poupon R. Assessment of biliary fibrosis by transient elastography in patients with PBC and PSC. Hepatology 2006; 43: 1118-1124.
[11] Haque M, Robinson C, Owen D, Yoshida EM and Harris A. Comparison of acoustic radiation force impulse imaging (ARFI) to liver biopsy histologic scores in the evaluation of chronic liver disease: A pilot study. Ann Hepatol 2010; 9: 289-293.
[12] Kettaneh A, Marcellin P, Douvin C, Poupon R, Ziol M, Beaugrand M and de Ledinghen V. Features associated with success rate and performance of FibroScan measurements for the diagnosis of cirrhosis in HCV patients: a prospective study of 935 patients. J Hepatol 2007; 46: 628-634.
[13] Kim BK, Han KH, Park JY, Ahn SH, Chon CY, Kim JK, Paik YH, Lee KS, Park YN and Kim do Y. A novel liver stiffness measurement-based prediction model for cirrhosis in hepatitis B patients. Liver Int 2010; 30: 1073-1081.
[14] Sandrin L, Fourquet B, Hasquenoph JM, Yon S, Fournier C, Mal F, Christidis C, Ziol M, Poulet B, Kazemi F, Beaugrand M and Palau R. Transient elastography: a new noninvasive method for assessment of hepatic fibrosis. Ultrasound Med Biol 2003; 29: 1705-1713.
[15] Wong VW, Vergniol J, Wong GL, Foucher J, Chan HL, Le Bail B, Choi PC, Kowo M, Chan AW, Merrouche W, Sung JJ and de Ledinghen V. Diagnosis of fibrosis and cirrhosis using liver stiffness measurement in nonalcoholic fatty liver disease. Hepatology 2010; 51: 454-462.
[16] Wang J, Ai H and Shi XY. Research program of ultrasonic elastography applied to hepatic fibrosis diagnosis. Chin J Ultrasonograph 2010; 19: 815-818.
[17] Gietka-Czernel M, Kochman M, Bujalska K, Stachlewska-Nasfeter E and Zgliczynski W. Real-time ultrasound elastography - a new tool for diagnosing thyroid nodules. Endokrynol Pol 2010; 61: 652-657.
[18] Zhang X, Xiao Y, Zeng J, Qiu W, Qian M, Wang C, Zheng R and Zheng H. Computer-assisted assessment of ultrasound real-time elastography: Initial experience in 145 breast lesions. Eur J Radiol 2014; 83: e1-7.
[19] Xu YX, Jia CM, Chen W, Li C, Hao YH, Chen M and Guo XH. Real-time tissue elastography with tissue dispersion quantitative analysis technique for assessment of rat liver fibrosis. Chin J Ultrasonograph 2013; 22: 893-896.
[20] Lin SH, Ding H, Mao F, Xue LY, Lv WW, Zhu HG, Huang BJ and Wang WP. Non-invasive assessment of liver fibrosis in a rat model: shear wave elasticity imaging versus real-time elastography. Ultrasound Med Biol 2013; 39: 1215-1222.
[21] Tamaki N, Kurosaki M, Matsuda S, Nakata T, Muraoka M, Suzuki Y, Yasui Y, Suzuki S, Hosokawa T, Nishimura T, Ueda K, Tsuchiya K, Nakanishi H, Itakura J, Takahashi Y, Matsunaga K, Taki K, Asahina Y and Izumi N. Prospective comparison of real-time tissue elastography and serum fibrosis markers for the estimation of liver fibrosis in chronic hepatitis C patients. Hepatol Res 2013; [Epub ahead of print].
[22] Tomeno W, Yoneda M, Imajo K, Suzuki K, Ogawa Y, Shinohara Y, Mawatari H, Fujita K, Shibata W, Kirikoshi H, Maeda S, Nakajima A and Saito S. Evaluation of the Liver Fibrosis Index calculated by using real-time tissue elastography for the non-invasive assessment of liver fibrosis in chronic liver diseases. Hepatol Res 2013; 43: 735-742.